



## Phylogenomic analysis reveals the evolutionary history of Palearctic needle-leaved junipers

David Gutiérrez-Larruscain<sup>a,\*</sup>, Pablo Vargas<sup>b</sup>, Mario Fernández-Mazuecos<sup>c</sup>, Juli G. Pausas<sup>a</sup>

<sup>a</sup> Department of Ecology and Global Change, Desertification Research Centre (CIDE: CSIC-UV-GVA), Valencia, Spain

<sup>b</sup> Department of Biodiversity and Conservation, Real Jardín Botánico (RJB: CSIC), Madrid, Spain

<sup>c</sup> Department of Biology (Botany), Faculty of Sciences, Universidad Autónoma de Madrid (UAM), Madrid, Spain

### ARTICLE INFO

#### Keywords:

Juniperus  
GBS  
Phylogeny  
Biogeography  
East Asian-Tethyan  
Taxonomy

### ABSTRACT

Needle-leaved junipers (*Juniperus* sect. *Juniperus*, Cupressaceae) are coniferous trees and shrubs with red or blue fleshy cones. They are distributed across Asia, Macaronesia and the Mediterranean Basin, with one species (*J. communis*) having a circumboreal distribution. Here we aim to resolve the phylogeny of this clade to infer its intricate evolutionary history. To do so, we built a comprehensive, time-calibrated phylogeny using genotyping-by-sequencing (GBS) and combine it with species occurrence using phylogeographic tools. Our results provide solid phylogenetic resolution to propose a new taxonomic classification and a biogeographical history of the section. Specifically, we confirm the monophyly of two groups within *J. sect. Juniperus*: the Asian (blue-cone) species including the circumboreal *J. communis*, and the Mediterranean-Macaronesian (red-cone) species. In addition, we provide strong phylogenetic evidence for three distinct species (*J. badia*, *J. conferta*, *J. lutchuensis*) previously considered subspecies or varieties, as well as for the differentiation between the eastern and western Mediterranean lineages of *J. macrocarpa*. Our findings suggest that the Mediterranean basin was the primary center of diversification for *Juniperus* sect. *Juniperus*, followed by an East Asian-Tethyan disjunction resulting from uplifts of the Qinghai-Tibetan Plateau and climatic shifts. The colonization history of Macaronesia by red-cone junipers from the western Mediterranean appears to have taken place independently in two different geological periods: the Miocene (Azores) and the Pliocene (Madeira-Canary Islands). Overall, genomic data and phylogenetic analysis are key to consider a new taxonomic proposal and reconstruct the biogeographical history of the iconic needle-leaved junipers across the Palearctic.

### 1. Introduction

The study of natural groups of related species that are significantly separated—geographically—has captured the attention of many scientist (Raven, 1972; Axelrod, 1975) since the development of biogeography in the 19th century (Nelson, 1978; Bueno-Hernández et al., 2023). Disjunct distributions have been explained by biological processes such as diversification following dispersion events (McDowall, 1978; Queiroz, 2005) or range contraction and habitat fragmentation leading to vicariance (Nelson & Platnick, 1981; Wiley, 1988). Additionally to the use of floristic, ecological, paleontological and paleogeographical data, the irruption of molecular techniques at the end of the last century has promoted the integration of phylogenetics into a biogeographical framework (Emerson & Hewitt, 2005).

Several phylogeographic studies have focused on broad

discontinuities between related Palearctic taxa distributed in East Asia and the Mediterranean basin (Chen et al., 2014; Xie et al., 2014; Valcarcel et al., 2017; Jiang et al., 2019; Xia et al., 2022). This distribution pattern is usually named East Asian-Tethyan disjunction. It was traditionally explained (Axelrod, 1975) as remnants of a subhumid, evergreen sclerophyllous vegetation belt placed across all Eurasia by the middle Eocene. However, more recent studies (Chen et al., 2014; Xie et al., 2014; Valcarcel et al., 2017; Jiang et al., 2019; Xia et al., 2022) suggested a more complex scenario in which long distance dispersal (LDD) and vicariance have played an important role in the establishment of East-Asian Tethyan disjunctions. One paradigmatic example of East Asian-Tethyan distributed species in Gymnosperms is the case of the needle-leaved junipers.

Junipers (*Juniperus* L., Cupressaceae) are evergreen coniferous trees or shrubs with fleshy cones that occur across the Northern Hemisphere

\* Corresponding author.

E-mail address: [david.gutierrez-larruscain@ext.uv.es](mailto:david.gutierrez-larruscain@ext.uv.es) (D. Gutiérrez-Larruscain).

<https://doi.org/10.1016/j.ympev.2024.108162>

Received 7 May 2024; Received in revised form 10 July 2024; Accepted 24 July 2024

Available online 26 July 2024

1055-7903/© 2024 The Authors. Published by Elsevier Inc. This is an open access article under the CC BY license (<http://creativecommons.org/licenses/by/4.0/>).

(with one species in eastern Africa). They have a deep history of diversification across wide range of ecological settings from dry ecosystems at the sea level to the top of mountains. The prevalent understanding is that the genus is composed of three sections (*Juniperus* sect. *Juniperus*, *J.* sect. *Sabina* Spach, and *J.* sect. *Caryocedrus* Endl.; Endlicher, 1847), although some authors considered them different genera (Antoine 1857, Wen-tsai et al., 1978; Yang et al., 2022). With a somatic chromosome number of  $2n = 22$ , polyploidy has only been documented in taxa belonging to *J.* sect. *Sabina*, with at least 10 polyploidization events reported across its evolutionary history (Farhat et al., 2019; 2023).

The species included in *J.* sect. *Juniperus* are distributed across the Palearctic and are easily recognized by their adult needle-type leaves articulated at the base and inserted at the stem in whorls of three (Adams, 2011). Currently, two classifications are widely followed (Table 1). The most conservative one is based on a thorough study of morphological characters and biogeographical patterns (Farjon 2001, 2017) and classified the section into 16 taxa within 7 species. The other classification (Adams 2011) is based on the analysis of phytochemical and molecular markers (Adams & Demeke, 1993; Adams, 2000; Adams et al., 2005; Adams et al., 2010; Mao et al., 2010; Adams, 2011; Adams & Schwarzbach, 2012) and classified the section into 24 taxa within 14 species (Table 1). Both classifications recognized two distinct morphological groups within the section. The first one has blue mature cones (galbuli), and includes *J. communis* and its allies (hereafter Blue Cone species *sensu* Adams & Schwarzbach 2012). The second group has red mature cones and includes *J. oxycedrus* and allies (hereafter Red Cone species *sensu* Adams & Schwarzbach 2012). The two groups have also distinct distributions. Blue Cone species—with the exception of the circumboreal *J. communis*—are distributed across Asia, from the east of

the Tibetan Plateau to the Japanese archipelagos, and from Primorye to Taiwan. Red Cone species are distributed throughout the Mediterranean basin and the Macaronesian archipelagos. Thus SE Asia and the Mediterranean-Macaronesian region are two hotspots of needle-leaved junipers connected by *J. communis*. Except for island endemics (i.e. *J. brevifolia* and *J. cedrus*), the Red Cone species have historically been regarded as subspecies or varieties of *J. oxycedrus*. In contrast, Adams et al. (2005) described *J. deltoides* as a cryptic species encompassing all the plants previously named under *J. oxycedrus* from the eastern Mediterranean region.

Mao et al. (2010) hypothesized an Euro-Asiatic origin for the genus *Juniperus* as a member of the Eocene Tethyan vegetation (Axelrod, 1975). The current Mediterranean distribution of sect. *Caryocedrus*, the early-diverging clade V of sect. *Sabina*, and the Mediterranean representatives of *J.* sect. *Juniperus* point to Europe as a plausible area of origin for the genus (Mao et al., 2010). The absence of Asian fossils of *J.* sect. *Juniperus* supports the idea of long-distance dispersal as a likely explanation for the former East Asian-Tethyan (east–west) disjunction between the Red and Blue Cone species, currently connected by *J. communis*.

Previous attempts to elucidate the phylogenetic and biogeographical history of *J.* sect. *Juniperus* (Adams, 2000; Martínez-Rodríguez & Vargas, 2022; Adams & Schwarzbach, 2012; Rumeu et al., 2014) used conventional molecular markers based on Sanger sequencing. This approach did not provide enough resolution to resolve the phylogeny, and thus we lack an understanding of the evolutionary history of this clade. Several studies have demonstrated the use of genotyping-by-sequencing (hereafter GBS), a technique based on next-generation sequencing (Elshire et al., 2011), to improve phylogenetic resolution in different plant clades (Escudero et al., 2014; Hamon et al., 2017; Fernández-Mazuecos et al., 2018; Martín-Hernanz et al., 2019; Liang et al., 2021; Uckele et al., 2021; Otero et al., 2022). Here we propose to use GBS to generate a fully resolved and dated phylogeny of *J.* sect. *Juniperus* with the following aims: (1) explore the biogeographical history and the origin of the two juniper hotspots (East Asia and the Mediterranean Basin), as a paradigmatic example of East Asian-Tethyan distributed species in Gymnosperms; (2) test the monophyly of the Red Cone and the Blue Cone species groups; and (3) resolve the phylogenetic relationships within the *J.* sect. *Juniperus* and shed light on the taxonomic status of its ascribed taxa.

## 2. Material & methods

### 2.1. Plant material, library preparation and sequencing

Dry plant material (herbarium records and field collections) from 51 individuals corresponding to 25 taxa were processed for inclusion in the GBS analysis. The ingroup consisted of 30 individuals corresponding to 15 taxa, which encompassed all the currently accepted (according to Farjon, 2017) species belonging to *Juniperus* sect. *Juniperus*. The outgroup comprised 21 individuals corresponding to 10 taxa, including samples from representative species of *J.* sect. *Sabina*, along with *J. drupacea* Labill. (the only member of *J.* sect. *Caryocedrus*), *Calocedrus decurrens* (Torr.) Florin, *Chamaecyparis lawsoniana* (A. Murray bis) Parl., *Cupressus sempervirens* L., *Platycladus orientalis* (L.) Franco and *Tetraclinis articulata* (Vahl) Mast. Additional information regarding the samples included in the analysis is available in Table S1.

Total genomic DNA was isolated following the CTAB protocol (Doyle & Doyle 1987) with minor modifications. These included 1) homogenizing 20–30 mg of dry leaf material in a bead mill tissue homogenizer; 2) adding PVP-40 to the isolation buffer (final concentration 0.04 %); and 3) addition of two 30 min incubation steps a  $-4^{\circ}\text{C}$  after the chloroform-isoamyl alcohol extraction and isopropanol precipitation steps. DNA concentration for each sample was measured using a double-strand broad-range Qubit 3.0 fluorometer assay (Life Technologies, Carlsbad, CA, USA). Genotyping-by-sequencing library construction was

**Table 1**

The two main taxonomic classifications of *J.* sect. *Juniperus* proposed by Adams & Schwarzbach (2012) and Farjon (2017) together with our proposal. Varieties of *Juniperus communis* were not considered in this study.

	Adams & Schwarzbach	Farjon	Proposal	
<b>Blue Cone species</b>	<i>J. communis</i> L.	<i>J. communis</i> L.	<i>J. communis</i> L.	
	<i>J. formosana</i> Hayata	<i>J. formosana</i> Hayata	<i>J. formosana</i> Hayata	
	<i>J. jackii</i> (Rehder) R. P. Adams	<i>J. communis</i> L.	–	
	<i>J. lutchuensis</i> Koidz.	<i>J. taxifolia</i> Hook. & Arn.	<i>J. lutchuensis</i> Koidz.	
	<i>J. mairei</i> Lemée & H. Lév.	<i>J. formosana</i> Hayata	<i>J. mairei</i> Lemée & H. Lév.	
	<i>J. rigida</i> var. <i>rigida</i> Siebold & Zucc.	<i>J. rigida</i> subsp. <i>rigida</i> Siebold & Zucc.	<i>J. rigida</i> Siebold & Zucc.	
	<i>J. rigida</i> var. <i>conferta</i> (Parl.) Patschke	<i>J. rigida</i> subsp. <i>conferta</i> (Parl.) Kitam.	<i>J. conferta</i> Parl.	
	<i>J. taxifolia</i> Hook. & Arn.	<i>J. taxifolia</i> Hook. & Arn.	<i>J. taxifolia</i> Hook. & Arn.	
	<b>Red Cone species</b>	<i>J. brevifolia</i> (Seub.) Antoine	<i>J. brevifolia</i> (Seub.) Antoine	<i>J. brevifolia</i> (Seub.) Antoine
		<i>J. cedrus</i> Webb & Berthel	<i>J. cedrus</i> Webb & Berthel	<i>J. cedrus</i> Webb & Berthel
<i>J. deltoides</i> R.P. Adams		<i>J. oxycedrus</i> subsp. <i>oxycedrus</i> L.	<i>J. deltoides</i> R.P. Adams	
<i>J. maderensis</i> (Menezes) R.P. Adams		<i>J. cedrus</i> Webb & Berthel	<i>J. maderensis</i> (Menezes) R.P. Adams	
<i>J. macrocarpa</i> Sm.		<i>J. oxycedrus</i> subsp. <i>macrocarpa</i> (Sm.) Neill.	<i>J. macrocarpa</i> Sm. s. l.	
<i>J. navicularis</i> Gand.		<i>J. oxycedrus</i> subsp. <i>transtagana</i> Franco	<i>J. navicularis</i> Gand.	
<i>J. oxycedrus</i> L.		<i>J. oxycedrus</i> subsp. <i>oxycedrus</i> L.	<i>J. oxycedrus</i> L.	
<i>J. oxycedrus</i> L.		<i>J. oxycedrus</i> subsp. <i>badia</i> (H. Gay) Debeaux	<i>J. badia</i> (H. Gay) Rivas Mart. et al.	

conducted following Fernández-Mazuecos et al. 2018 (adapted from Elshire et al. 2011, and Escudero et al. 2014). Briefly, 500 ng of DNA from each sample were digested using the PstI-HF restriction enzyme (New England Biolabs, Ipswich, MA, USA). After ligation to the bar-coded and common adapters, 5 µl of each sample were pooled, and the pool was purified using 1:1 AMPure XP beads (Beckman Coulter, Brea, CA, USA). Subsequently, 35 ng of the purified product were used for PCR amplification to enrich the library. After an additional purification step with 1:0.8 AMPure XP beads, quality control was performed using a Bioanalyzer 2100 (Agilent, Santa Clara, CA, USA). The single index library was then sequenced by Macrogen (Korea, Seoul) in one lane of 150-bp paired-end Illumina HiSeq X sequencing (Illumina, Inc., San Diego, CA, USA).

Raw data for the 51 individuals were deposited at the NCBI SRA database under BioProject PRJNA1083777.

## 2.2. Assembly and data processing

Raw FASTQ files were assembled by running the seven steps of the ipyrad 0.9.92 pipeline (Eaton & Overcast, 2020) on a High Performance Computer (HPC: Drago – CSIC). The ipyrad pipeline has demonstrated its efficiency in the assembly of restriction site-associated NGS data and is widely employed in phylogenomic studies (Fernández-Mazuecos et al. 2018, Martín-Hernanz et al. 2019, Wagner et al. 2020, Hühn et al. 2022). One of its advantages is that it allows for indel variation, which is frequent in phylogenetic datasets (Shafer et al., 2017; Eaton & Overcast, 2020). Ipyrad provides the option to assemble datasets using either *de novo* or *reference*-based methods, as well as the option of *de novo* – *reference* (i.e., retaining only those sequences not matching the reference genome).

Since employing a reference genome is theoretically better for ensuring orthology of the assembled loci, we utilized the plastid genome of *Juniperus sabina* (Almerikova et al. 2022; GeneBank ID: OL467323), and the complete genome of *Cupressus sempervirens* (GeneBank ID: GCA\_028749045.1) as reference genomes. To evaluate the performance of various assembly strategies, we employed two different approaches: (1) *de novo* – *reference* assembly, removing those reads mapped against the plastid genome of *J. sabina* and then assembling the remaining reads *de novo*; and (2) *reference* mapping against the *C. sempervirens* genome. In the latter, we specifically utilized scaffolds corresponding to eleven annotated chromosomes to prevent reference mapping against non-nuclear DNA.

Default ipyrad parameters were adjusted to allow a single nucleotide mismatch in barcodes and trimming the first five base pairs of each read. Starting from 141,157,682 raw reads, we evaluated several clustering threshold (CT) values ranging from 0.81 to 0.97 and minimum sample counts per locus (M) from 5 to 25, resulting in 50 analyzed assemblies (Notes S1, Figures S1, S2, S3 in Supplementary Material). Of these, we selected two for further phylogenetic analysis. From the *de novo* approach, we selected the CT=0.91, M=25 assembly (hereafter *de novo*-based or *de novo* dataset). This choice was made because this dataset represented a good balance between the number of parsimony-informative sites (hereafter PIS) and the proportion of missing data in the final alignment (2962 loci; 36,884 PIS in a 432113-bp alignment with a total of 39.08 % missing sites; Fig. S3). From the *reference* approach, we opted for M=25 (hereafter *reference*-based or *reference* dataset) as it exhibited the lowest amount of missing sites among the *reference*-based assemblies (4392 loci; 109,699 PIS in a 1429270-bp alignment with a total of 57.80 % missing sites; Fig. S3).

## 2.3. Phylogenetic analyses

To explore the phylogenetic relationships among the species of *J. sect. Juniperus*, we employed a combination of a super-matrix concatenation approach and a multispecies coalescent (MSC) method.

For the concatenated super-matrix approach, we conducted a

Bayesian inference phylogenetic analysis using the software MrBayes 3.2.7 (Ronquist et al., 2012; Ayres et al., 2012). We set the number of substitution types to 6, corresponding with the GTR model, with a gamma-distributed rate variation and a proportion of invariant sites (invgamma). We set two independent runs of 4 chains, three of them heating at a temperature of 0.2. Each analysis was run for 5 million generations, with trees sampled every 10,000 generations. After checking the average standard deviation of split frequencies (<0.01) to assess run convergence, and reaching effective sample sizes bigger than 200, a majority-rule consensus tree was constructed discarding the first 25 % of sampled trees. Additionally, a maximum likelihood analysis was carried out on the concatenated matrices using IQ-TREE multicore version 2.2.2.7 (Minh et al., 2020a). The best-fitting substitution model for each locus was estimated using the *ModelFinder* algorithm (Kalyaanamoorthy et al., 2017) implemented in IQ-TREE. A partition model, as implemented in IQ-TREE (Chernomor et al., 2016) was utilized for setting independent evolutionary rates and branch lengths to each partition. Branch support values were estimated by running 1000 iterations of ultrafast bootstrap (UFBoot; Hoang et al., 2018) and 1000 iterations of SH-like approximate likelihood ratio test (SH-aLRT; Guindon et al., 2010).

To infer species-level phylogenies under the MSC model, we employed a summary method, which involves reconstructing a species tree from a set of gene trees. To achieve this, we first reconstructed maximum likelihood phylogenetic trees for each locus per assembly using the software IQ-TREE. Branch support values for every maximum likelihood gene tree were estimated by running 1000 iterations of UFBoot. To address the sensitivity of summary methods to the quality of input gene trees, we applied a branch-collapsing procedure. Removing branches with low support helped reduce potential noise in the species tree reconstruction. All branches with UFBoot values lower than 30 were collapsed using the TreeCollapseCL4 JavaScript tool (<http://emmahodcroft.com/TreeCollapseCL.html>). Finally, we used the ASTRAL-III (Zhang et al., 2018) reconstruction method implemented in the JavaScript tools astral.5.7.8.jar to infer the species tree from the set of gene trees. Taxon coding was provided in order to obtain only one tip per species in the reconstructed tree; branch support was assessed by calculating branch local posterior probabilities (hereafter LPP; Sayyari & Mirarab, 2016).

In addition to the Bayesian posterior probabilities (hereafter BPP) calculated during the Bayesian inference analysis, gene concordance factors and site concordance factors (hereafter gCF and sCF, respectively; Minh et al., 2020b) were also estimated for the topology obtained through the concatenated supermatrix. gCF and sCF were calculated with the software IQ-TREE, using the sets of gene trees calculated for the summary method analysis, over the topology obtained from the phylogenetic Bayesian analysis.

Finally, to detect ancient hybridization events within *J. sect. Juniperus*, a phylogenetic explicit network based on maximum pseudolikelihood estimation was calculated using SNaQ (Solís-Lemus and Ané, 2016) pipeline implemented in the Julia package PhyloNetworks (Solís-Lemus et al., 2017). Gene trees from the *reference* dataset used as input to ASTRAL were pruned to ingroup species plus *J. drupacea*, over which 30 independent runs for each of up to 10 maximum hybridization events values (hereafter hmax) were calculated. After parameter optimization of the best network obtained from the 30 runs of each hmax value, the network scored with the best pseudo-deviance value was chosen as the optimum network.

## 2.4. Dating and historical biogeography

Divergence times for the topologies derived from the Bayesian inference analysis were estimated using RelTime (Tamura et al., 2012, 2018), an approach based on the relative rate framework (RRF) and implemented in the software MEGA11 (Molecular Evolutionary Genetic Analysis version 11; Tamura et al., 2021). One of the key advantages of

the RRF is its independence from assumptions about the statistical distribution of lineage rate variation. RelTime can incorporate calibration points as probabilities densities and has been demonstrated to perform efficiently for large molecular datasets with similar results as molecular dating methodologies based on Bayesian approaches, but with affordable calculation times (Costa et al., 2022). We run RelTime using the tree topology with branch lengths obtained from the Bayesian inference analysis, and set calibration points based on the fossil record (Table S2). To establish local clocks, the software applies Maximum likelihood statistical methods through the use of a General Time Reversible Model (GTR) with a Gamma distribution of rates among sites and proportion of invariants sites (+I).

To explore the impact of historical processes on current biodiversity patterns we conducted a historical biogeography analysis using the R package Herodotools (Nakamura et al., 2023). Herodotools integrates current species distribution, biogeographical regionalization, macro-evolutionary (phylogenetic) analysis, and ancestral range reconstruction models, from a presence-absence matrix based on a map (grid format) and a dated phylogeny.

Occurrence data for each taxon of *J. sect. Juniperus* included in our phylogeny, plus *J. drupacea*, were extracted from the Global Biodiversity Information Facility (GBIF; <https://doi.org/10.15468/dd.4ps5n7>), followed by manual curation and filtering (e.g. excluded those records that were clearly outside of the species distribution area). Due to the difficulty in accurately identifying occurrences solely based on the overlapping native ranges of *J. mairei* and *J. formosana*, which are synonymized in the GBIF database, *J. mairei* was excluded from this analysis. A presence-absence matrix was generated from the occurrence map (with 1.5° grid cells) using the R package letsR (Vilela & Villalobos, 2015). We employed the dated tree topology obtained from the *de novo* dataset using the RelTime procedure, after pruning tips to retain one sample per taxon and excluding *J. mairei* and the outgroup samples.

To identify geographic centers of evolutionary diversification in *Juniperus sect. Juniperus*, we performed a biogeographical regionalization (Maestri & Duarte, 2020) also using the Herodotools R package. Ancestral range reconstruction was executed using the six models implemented in the R package BioGeoBears (Matzke, 2014). Geographic areas were assigned based on the results of the regionalization analysis, except for *J. communis*, which was considered ubiquitous (except for region A, see Results). To incorporate the fossil evidence data of *J. drupacea* in the western Mediterranean area during the Miocene (Palamarev, 1989) into the analysis, we constrained the ranges at nodes according to BioGeoBears documentation. For that, we set the likelihood values at the split node of *J. drupacea* to 1 for the following ancestral range areas: 1) its current distribution area (A); 2) the region corresponding to the Mediterranean Basin (B); and 3) both of them (AB).

We selected the best-fitting model using AIC (Table S3) and computed different analyses at the assemblage level using Herodotools. Specifically, the age of each assemblage was estimated as the mean arrival time of the lineages currently distributed in each cell. This metric assumes a scenario where no further dispersal events occurred, as outlined by Van Dijk et al. (2021). We also estimated the contribution of each region to the current species distributions in each assemblage, interpreted as historical dispersal events.

### 3. Results

#### 3.1. Phylogenetic reconstructions

The Bayesian and maximum likelihood analyses derived from the super-matrix concatenation approach produced identical topologies for each dataset, and nearly identical topologies between datasets (Fig. S4). All the branches were strongly supported by high values of Bayesian posterior probabilities, UFBoot and SH-aLRT (Fig. S4). Values of gene and site concordance factors (gCF and sCF) for each branch were similar between the *de novo* topology (24.70 and 66.91) and the *reference*

topology (26.18 and 65.96, respectively). The sCF values for each branch were higher than the gCF values for both topologies, resulting in higher concordance factors for the longest branches (Fig. S4). Therefore, unless otherwise stated, the results are based on the *reference* topology, excluding the outgroup except for *J. drupacea* (Fig. 1).

The phylogenetic analysis recovered *Juniperus* as a monophyletic group comprising three clades (Fig. 1 and Fig. S4) corresponding with each of the three sections. *Juniperus sect. Sabina* was recovered as sister to the remaining sections, while *J. sect. Caryocedrus* and *J. sect. Juniperus* were sister to each other.

Within *J. sect. Juniperus*, Blue Cone species formed a monophyletic group (Fig. 1) that included *J. communis* in an early-diverging position with respect to the Far East group. The Chinese specimen of *Juniperus mairei* was recovered in a sister group relationship with the remaining taxa, which formed two sister subclades. The first one included *J. formosana* and *J. taxifolia*, specimens originally from Taiwan and Japan, respectively. The second one included individuals collected in Japan: *J. rigida*, which was recovered as sister to the clade composed by *J. conferta* and *J. lutchuensis*.

Red Cone species formed another monophyletic group (Fig. 1), sister to the Blue Cone group, and in turn, consisting of two sister lineages. The first one included three species: *J. brevifolia*, *J. navicularis* and *J. deltoides* (hereafter Clade BND). Within this clade, *J. brevifolia* and *J. navicularis* were recovered as sister taxa.

The second lineage within the Red Cone group (Fig. 1) consisted of *J. oxycedrus* and its closest relatives (*J. oxycedrus* clade). An eastern Mediterranean (Greece) specimen of *J. macrocarpa* was placed at an early-diverging position within this clade (hereafter *J. macrocarpa* EM lineage). Two western Mediterranean (Spain) specimens of *J. macrocarpa* (hereafter *J. macrocarpa* WM lineage) were recovered in a sister position to a clade containing two independent lineages. The first lineage includes Spanish samples of *J. oxycedrus* subsp. *oxycedrus*, while the second lineage comprises two clades. One consists of specimens of *J. cedrus* and *J. maderensis* in a sister relationship, while the other includes specimens of *J. badia*.

For the summary tree phylogenetic inference method, the two tree topologies obtained from the analyses of the *reference* and *de novo* datasets largely agreed (Fig. 2), and were generally consistent with the results of the concatenation-based phylogenetic analyses. The values of local posterior probability (LPP) were generally high (mostly above 90). However, there was topological incongruence in the phylogenetic position of *J. deltoides*, which was recovered in a sister position to *J. navicularis* in the reference-based topology, but with a low LPP support of 22. The relationships among Blue Cone species from the Far East were not fully resolved based on LPP values, particularly those between *J. rigida*, *J. lutchuensis*, *J. conferta* and the remaining species in the clade. Additionally, the summary method based on the *de novo* assembly did not fully resolve the phylogenetic relationships among *Cupressus*, *Juniperus*, and the clade including *Calocedrus*, *Tetraclinis*, and *Platycladus*.

The best-scored network from the SNaQ analysis was obtained from the hmax = 7 runs, revealing three gene transfer events (Fig. S5). An ancient hybridization event was detected from the ancestor of the *J. conferta* – *J. rigida* – *J. lutchuensis* clade towards ( $\gamma = 0.0934$ ) the stem of the Red Cone group. The remaining two events appear more recent than the latter one. The first involves transfer from *J. lutchuensis* lineage to *J. conferta* lineage ( $\gamma = 0.485$ ), and the second indicates transfer from *J. cedrus* – *J. maderensis* lineage to *J. brevifolia* lineage ( $\gamma = 0.28$ ).

#### 3.2. Dated phylogenies and historical biogeography

Divergence times estimated from both the *reference*- and *de novo*-based trees generally yielded similar results (Fig. 3A, Fig. S6, Fig. S7; Table 2). The divergence between *Juniperus* and *Cupressus* was estimated at 40.75/40.68 Ma (hereafter, the first and second values indicate the estimates from the *de novo* and *referenced*-based approaches respectively) and the crown clade of *Juniperus* at 28.07/27.88 Ma.

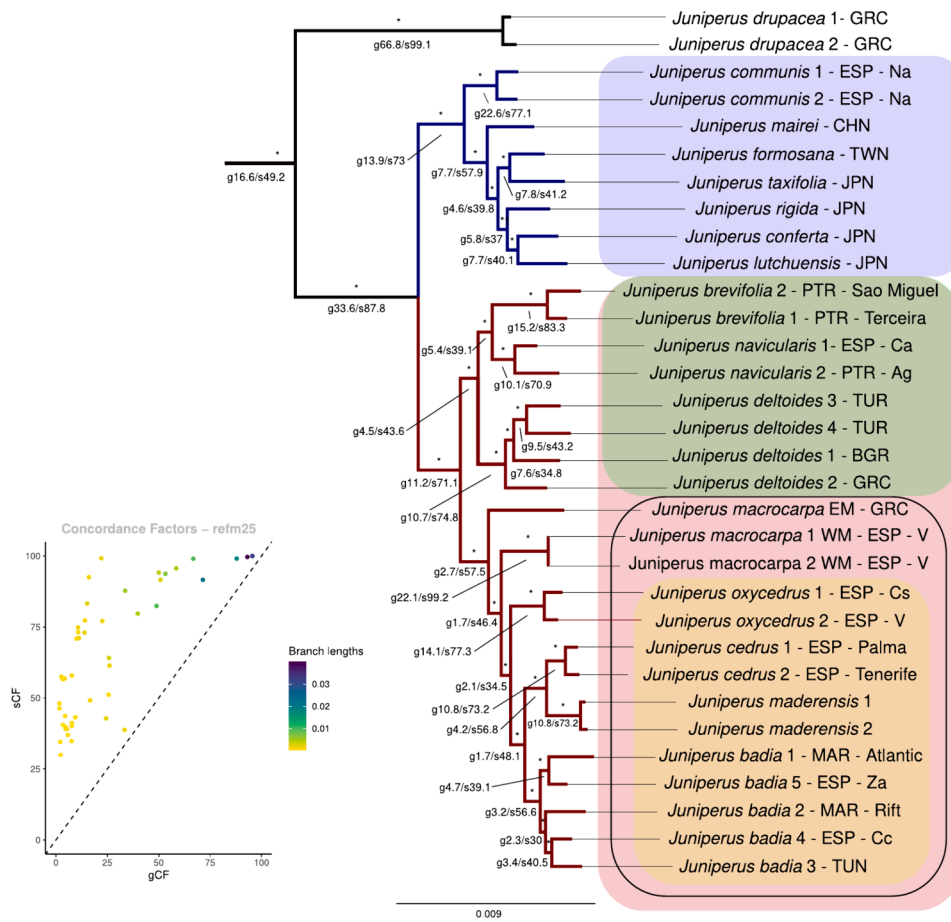


**Fig. 1.** Phylogenetic analysis using a concatenated Super-Matrix Approach derived from the *reference*-based dataset. Support values for branches are indicated above each branch, represented by Bayesian Posterior Probabilities (BPP), UltraFast Bootstrap (UFBoot), and Shimodaira-Hasegawa-like approximate likelihood ratio test (SH-aLRT) values, respectively. Asterisks (\*) denote instances where all support values reach 100%. Below the branches, concordance factors are detailed, with general Concordance Factors (gCF) and specific Concordance Factors (sCF) provided. Color coding is as follows: Blue for the BSC clade, Red for the RSC clade, Green for the BND clade, with the *J. oxycedrus* clade marked by a black rectangle, and the *J. oxycedrus* and allies group highlighted in orange. (For interpretation of the references to color in this figure legend, the reader is referred to the web version of this article.)

We detected two diversity centers for *J. sect. Juniperus*: the Mediterranean basin and the Sino-Japanese region (Fig. 3B). We also identified four distinct evolutionary regions (Fig. 3C): region A is a small region in the Hellenic peninsula and western Asia, corresponding to the current distribution of *J. drupacea*; region B encompasses nearly the entire Mediterranean Region plus Macaronesia; region C includes a portion of the Sino-Japanese region; and region D reflects the circum-boreal range of *J. communis*.

Among the six tested biogeographical models, AIC values favored the DEC (Dispersal-Extinction-Cladogenesis) model (Fig. 3A). The ancestral range estimation analysis suggested regions A or B as the possible ancestral range for the most recent common ancestor of *J. sect. Caroycedrus* and of *J. sect. Juniperus*, dated at 23.72/23.95 Ma. The most likely ancestral range at the crown node of *J. sect. Juniperus*, dated at 15.24/15.01 Ma, was region B, with a smaller probability for region C. The ancestor of the Blue Cone group could have been distributed in regions B, C, or a combination of B and D (Fig. 3A). The ancestor of the Red Cone group likely remained in region B, with recent dispersal events explaining the colonization of the Macaronesian archipelago. As a consequence, the mean arrival time of lineages to each assemblage (Fig. 3D) could be categorized into three ranges similar to the defined evolutionary regions: the oldest one includes most of the assemblages corresponding to region B; the mid-age one comprises region C; and the most recent one corresponds to assemblages distributed across region D. The major dispersal contribution from region B (Fig. S8A) involves

assemblages distributed in regions A and C. The dispersal contribution of region C (Fig. S8B) corresponds to the current distribution of *J. communis*, including all assemblages of region D, and parts of regions B and C.

## 4. Discussion

### 4.1. GBS phylogenomics and a taxonomic proposal within *J. Sect Juniperus*

The analysis of genotyping-by-sequencing (GBS) data has provided a fully resolved phylogeny of *Juniperus sect. Juniperus*. There were no substantial differences between the analyses of the *reference* and *de novo* datasets, despite the considerable gap in the number of loci recovered, but the *reference* approach proved advantageous in yielding a higher number of informative loci (Notes S2 *insupplementary material*). Thus, there is robust evidence for the reliability of our phylogeny, which provides new insights into the systematics of needle-leaved junipers.

We found strong support for the monophyly of the section (Mao et al., 2010; Adams & Schwarzbach, 2012; Adams & Schwarzbach, 2013; Uckele et al., 2021) and provided the first phylogenetic evidence supporting both the Blue Cone (Rumeu et al., 2011, 2014; Adams & Schwarzbach, 2012, 2013) and Red Cone groups as independent evolutionary lineages.

Our phylogeny positioned *J. communis* in an early-diverging branch

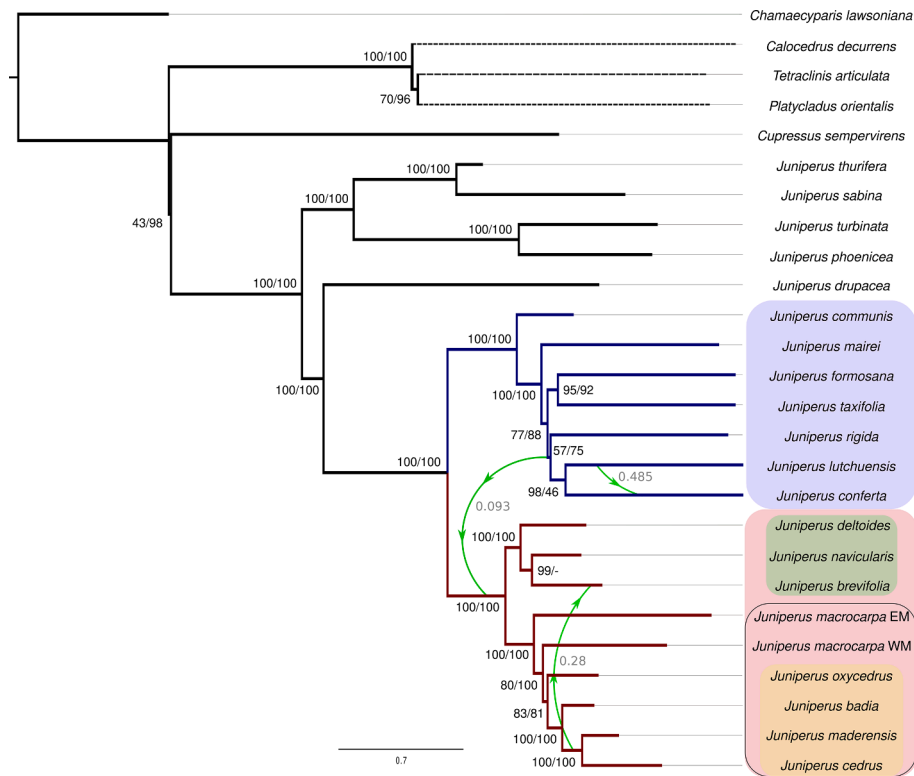


**Fig. 2.** Species Tree analysis based on a Summary method. Numbers at the branches represent local posterior probabilities: at the left correspond to the support values obtained from the analysis of the *denovo*-based dataset, while the numbers to the right reflect support values from the analysis of the *reference* dataset. Green lines with arrows indicate reticulation events obtained from the explicit network analysis. Grey numbers represent inference values ( $\gamma$ ) from each parental. Color coding: Blue for the BSC clade, Red for the RSC clade, Green for the BND clade. The *J. oxycedrus* clade is marked by a black rectangle, and the *J. oxycedrus* and allies group is highlighted in orange. (For interpretation of the references to color in this figure legend, the reader is referred to the web version of this article.)

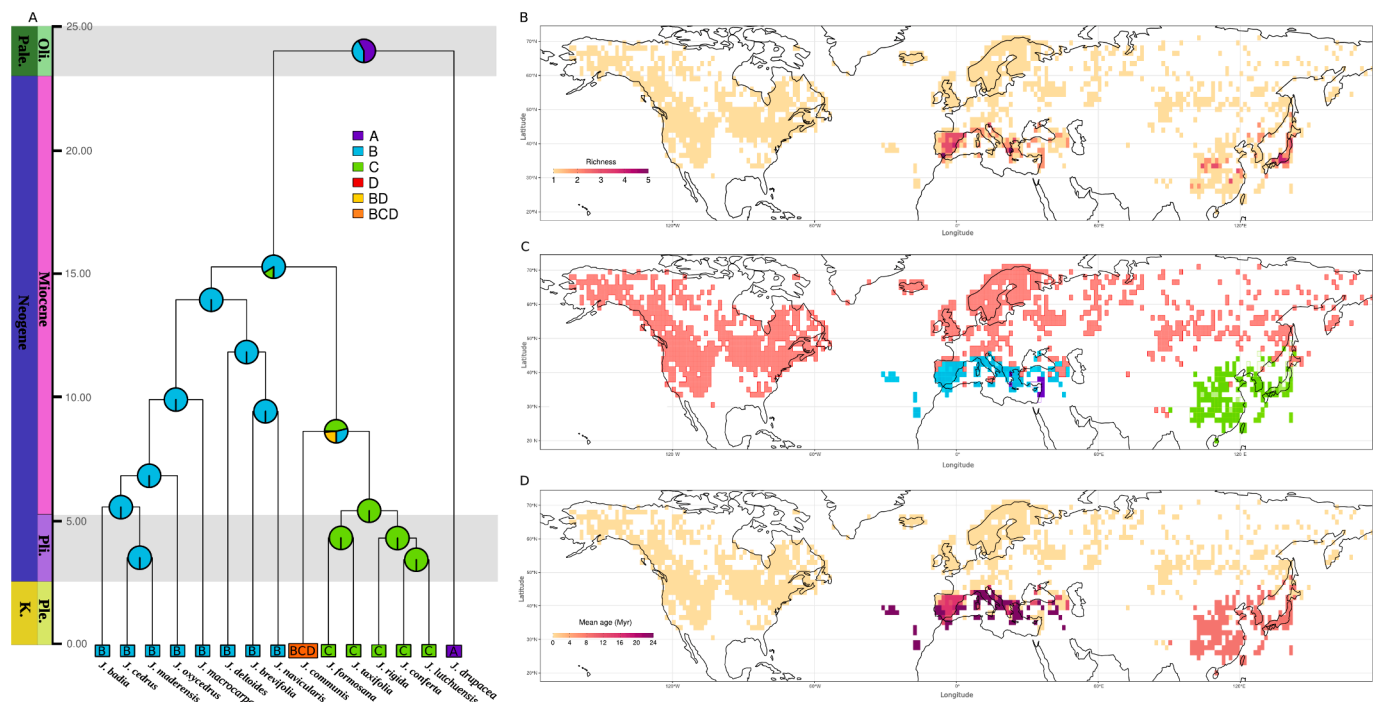


**Fig. 3.** Comprehensive historical biogeography analysis of *Juniperus* sect. *Juniperus* and *J. drupacea*: A) Ancestral range reconstruction, with areas A, B, C and D corresponding to those identified in Fig.3C; B) Species richness map; C) Results of a regionalization analysis; D) Arrival time map, where the color gradient indicates the mean arrival time of lineages at each assembly.

**Table 2**

Divergence times at each node for the dated phylogenies based on the relative rate framework (RRF). Confidence intervals are provided in brackets.

Node	Reference-based analysis (Myr.)	De novo-based analysis (Myr.)
Split of <i>Cupressus</i>	(59.21) – 40.68 – (35.26)	(51.1) – 40.75 – (32.5)
Crown of <i>Juniperus</i>	(32.06) – 27.88 – (24.76)	(31.5) – 28.07 – (25.01)
Crown of <i>J. sect. Sabina</i>	(29.55) – 24.76 – (24.76)	(28.55) – 24.79 – (24.79)
Split <i>J. sabina</i> & <i>J. thurifera</i>	(15.91) – 11.9 – (8.89)	(16.34) – 12.12 – (8.99)
Split <i>J. phoenicea</i> & <i>J. turbinata</i>	(12.78) – 9.44 – (6.97)	(12.16) – 9.23 – (7.01)
Split <i>J. sect. Caryocedrus</i>	(32.06) – 23.72 – (16.97)	(30.4) – 23.95 – (18.86)
Crown <i>J. sect. Juniperus</i>	(16.99) – 15.01 – (13.93)	(16.78) – 15.24 – (13.91)
Crown RSC clade	(14.37) – 13.94 – (13.93)	(14.35) – 13.91 – (13.91)
Crown BND clade	(12.2) – 11.55 – (10.94)	(12.36) – 11.8 – (11.27)
Split <i>J. brevifolia</i> & <i>J. navicularis</i>	(10.56) – 9.53 – (8.61)	(10.2) – 9.41 – (8.69)
Crown <i>J. oxycedrus</i> clade	(11.07) – 10 – (9.03)	(10.7) – 9.89 – (9.13)
Split of <i>J. macrocarpa</i> WM	(9.61) – 8.18 – (6.96)	(8.82) – 7.77 – (6.85)
Split <i>J. oxycedrus</i>	(8.54) – 7.03 – (5.79)	(7.94) – 6.82 – (5.85)
Split <i>J. badia</i>	(6.99) – 5.61 – (4.5)	(6.61) – 5.55 – (4.66)
Split <i>J. cedrus</i> & <i>J. maderensis</i>	(4.79) – 3.5 – (2.55)	(4.49) – 3.51 – (2.74)
Crown BSC clade	(14.36) – 8.93 – (5.55)	(12.13) – 8.61 – (6.11)
Split <i>J. mairei</i>	(9.56) – 6.51 – (4.43)	(8.29) – 6.25 – (4.71)
Crown East Asian BSC representatives	(8.79) – 5.5 – (3.44)	(7.64) – 5.4 – (3.82)
Split of <i>J. rigida</i>	(7.86) – 4.67 – (2.77)	(6.34) – 4.3 – (2.92)
Split <i>J. formosana</i> & <i>J. taxifolia</i>	(7.48) – 4.33 – (2.51)	(6.47) – 4.31 – (2.87)
Split <i>J. conferta</i> & <i>J. lutchuensis</i>	(6.9) – 3.79 – (2.08)	(5.38) – 3.43 – (2.19)

of the Blue Cone clade, as sister to East Asian species, in contrast to previous work using a few less informative markers that suggested *J. taxifolia* closer to *J. communis* than to the rest of the Asian-restricted species (Mao et al., 2010; Rumeu et al., 2011; Adams & Schwarzbach, 2012; Adams & Schwarzbach, 2013; Rumeu et al., 2014). Additionally, incomplete lineage sorting (Naciri and Linder, 2015) or introgression between ancestral *Juniperus* lineages may have affected previously published phylogenetic reconstructions based on plastid markers (Li et al., 2022; Steenwyk et al., 2023).

Our analyses consistently recovered *J. lutchuensis* and *J. conferta* in a sister relationship (Fig. 1) and closely related to *J. rigida* (Figs. 1, 2) which contrast with previous research (Table 1). Despite the gene transfer event detected between both lineages (Fig. 2), which could explain they shared prostrate-decumbent habit and coastal sandy and rocky habitats, they can be morphologically distinguished by the number of stomatal bands on the adaxial leaf surface (i.e., two in *J. lutchuensis*, one in *J. conferta*; Adams, 2014). Thus, we consider *J. conferta* as an independent lineage from *J. rigida* as *J. lutchuensis* from *J. taxifolia* (Table 1).

In relation to the Red Cone clade, our phylogeny also supports the two distinct lineages: the BND clade (*J. brevifolia*, *J. navicularis* and *J. deltooides*) and the *J. oxycedrus* clade (Figs. 1, 2), as suggested in previous studies (Table 1; Rumeu et al., 2011, 2014; Adams & Schwarzbach, 2012). In the *J. oxycedrus* clade, *J. macrocarpa* was consistently recovered as paraphyletic (Figs. 1, 2), with an early diverging branch corresponding to a sample from Greece (referred to as the eastern Mediterranean lineage in our analysis; *J. macrocarpa* EM) and a later branch with the western samples. This great differentiation between eastern and western lineages of *J. macrocarpa* mirrors the pattern of species-level differentiation between *J. deltooides* and *J. oxycedrus* (Adams et al., 2005). If both lineages of *J. macrocarpa* were considered distinct species, the name *J. macrocarpa* would be reserved for the eastern

Mediterranean lineage, as the species was originally described by Smith in Sibthorp & Smith (1816) based on Greek plant material. For the western lineage, the preferred name would be *J. willkommii* Ant. as Antoine (1857) assigned this name to plant material collected in the same locality of our *J. macrocarpa* WM lineage (eastern coast of the Iberian Peninsula) by Willkomm (1852). However, our limited sampling of *J. macrocarpa* prevents us from proposing definitive taxonomic changes.

The last clade of the Red Cone group includes *J. oxycedrus* in a sister relationship to a clade formed by *J. badia* and the southernmost Macaronesian junipers: the Canarian *J. cedrus* and the Madeiran *J. maderensis*. We revealed, for the first time, a sister relationship of *J. cedrus* and *J. maderensis*, with a split in their evolutionary history dated to around 3.5 Ma (Figs. 1, 2, 3; Table 2). Additionally, we detected a possible gene transfer event from the southernmost Macaronesian junipers to the Azorean *J. brevifolia*, which explains the topological conflict at the species tree reconstruction (Fig. 2) between the *de novo* and reference datasets.

*Juniperus badia* was recently elevated to the species level (Rivas-Martínez et al., 2020) and identified as a juniper endemic to northern (Mediterranean) Africa, biogeographically related to the Iberian endemic taxon *J. oxycedrus* subsp. *lagunae* (Pau ex C. Vicioso) Rivas Mart. *Juniperus badia* was described as a variety of *J. oxycedrus* by Gay (1889) based on plant material from Algeria. Historically, all these plants were included within the variability of *J. oxycedrus* either as varieties or subspecies, with some molecular support (Adams & Schwarzbach 2012; Rumeu et al., 2011, 2014; Boratyński et al., 2014). Our reconstruction solved this long-standing controversy and suggests that *J. badia* is an independent lineage from *J. oxycedrus*, closely related to the clade comprising *J. cedrus* and *J. maderensis*. It diverged from *J. oxycedrus* ca. 7 Ma and subsequently from the Macaronesian taxa ca. 5.6 Ma. Despite some morphological differences reported from *J. oxycedrus* (Amaral Franco, 1986; Adams, 2011, Farjon 2017), such as broader leaves or larger purplish galbula in *J. badia*, these morphological traits often overlap. The distinct conic crown shape of *J. badia*, up to 15 m tall with subpendulous ultimate branchlets contrasts with the habit of *J. oxycedrus*, typically a shrub or a small tree that lacks subpendulous ultimate branchlets. The recovered clade including *J. badia* samples from Morocco, Tunisia, and the Iberian Peninsula (Fig. 1, Table S1) supports the recognition of *J. badia* at the species taxonomic level. This taxon must include the Iberian plants named *J. oxycedrus* subsp. *lagunae*.

#### 4.2. Biogeographic history of Blue Cone species and the East Asian-Tethyan connection

Mao et al. (2010) proposed that the genus *Juniperus* originated in the Eocene Tethyan vegetation (Axelrod, 1975), when laurophyllous forests transitioned to evergreen sclerophyllous vegetation along the shores of the Tethys Ocean (which spanned from the current Mediterranean basin to Central Asia). Farjon (2005) suggested that subsequent cooling and aridification during the Eocene-Oligocene transition favored the conifer expansion, while Mao et al. (2010) proposed higher diversification rates for *Juniperus* during the Miocene, coinciding with the crown age of *J. sect. Juniperus* (Fig. 3A). Evidence for the Miocene as an outstanding period of conifers diversification has also been documented (Zhao et al., 2024) in the clade that includes *Pinus* subsect. *Pinus* L., another iconic group of Eurasian Gymnosperms. Contrary to the idea of gymnosperms as “living fossils” (Crisp & Cook, 2011), relatively recent diversification events like those observed in *J. sect. Juniperus* may have emerged following extinction episodes associated with the global cooling during the Upper Cenozoic (Davis & Schaefer, 2011; Nagalingum et al., 2011; Condamine et al., 2020).

Miocene fossil records from Bulgaria and Georgia (Palamarev, 1989; Palamarev et al., 2005) suggest that the ancestor of *J. drupacea* (Syrian juniper) had a broader distribution encompassing the current eastern Mediterranean and western Asia. These data align with the ancestral

range reconstruction (Fig. 3A), which indicates the likely origin of the section in the Mediterranean Basin (areas A and B). These ancestral lineages likely spread from western Asia through Anatolia and Central Asia during the Miocene, reaching East Asia before the final uplift of the Tibetan Plateau in the late Neogene (Li et al., 2021; Spicer et al., 2021; Su et al., 2019). Jiang et al. (2019) proposed the existence of an Eurasian warm humid corridor during the Oligocene to the early Miocene along the margins of the Himalaya and Tibet, explaining the east–west dispersion of eastern oaks to the Mediterranean basin. Another possible way to the east, as suggested for *Atractylodes* lineages (Xia et al., 2022), is the Pamir Mountains route following the closure of the Turgai Strait in the late Oligocene. This alternative pathway, possibly drier than the latter, would have allowed migration directly through East Asia via the Mongolian Plateau.

Climatic changes induced by the final uplift of the Tibetan Plateau may have led to a habitat reduction and vicariance, generating the Eastern Asia–Tethyan disjunction for the ancestral lineages of *J. sect. Juniperus* (Tu et al., 2010; Chen et al., 2014; Xie et al., 2014; Deng et al., 2017; Xia et al., 2022). As a consequence, warmer and wetter conditions in East Asia (Liu and Yin, 2002; Zhang et al., 2016) could have facilitated their diversification into the current Blue Cone species. Although junipers present a zoochorous bird-mediated dispersal system, no evidence of post-vicariance LDD events within the Blue Cone lineage was detected in our study, unlike the cases of *Hedera* L. (Valcárcel et al., 2017) and *Pistacia* L. (Xie et al., 2014) where LDD facilitated subsequent species diversification events.

The crown node of this clade is younger (Late Miocene, 8.8 Ma) than the Mediterranean clade (Fig. 3A), and the dispersal contribution analysis (Fig. S8A) identified the Mediterranean Region (B) as the major contributor to the current assemblages in the Sino–Japanese area. Although no fossil records exist for *J. sect. Juniperus* in Asia, our results lead us to propose an ancient East Asian–Tethyan disjunction for the section that was subsequently bridged by the expansion of the circumboreally distributed *J. communis* (Fig. 3D). This connection between the Mediterranean basin and eastern Asia is also mirrored in the distribution pattern of *Pinus sylvestris* L. regarding to *P. subsect. Pinus* (Zhao et al., 2024), which like *J. communis* bridges two diversity hotspots (i.e. Mediterranean basin and eastern-southern Asia for *P. subsect. Pinus* species).

While one ancient *Juniperus* lineage led to the Blue Cone Sino–Japanese clade (area C) (Fig. 3A, C), another one—the ancestor of *J. communis*—, acquired enough plasticity (Tumajer et al., 2021) to become the most widely distributed conifer in the Northern Hemisphere (Farjon, 2017). Our findings support a rapid expansion of *J. communis* (Fig. 3D) around the Pliocene–Pleistocene, consistent with Mao et al. (2010), connecting the Mediterranean and the East Asia juniper groups. Dispersal contributor analysis (Fig. S8B) identifies the Sino–Japanese area (C) as the mayor contributor to the assemblages including *J. communis*, which corresponds to the circumboreal area representing the current distribution of the common juniper (D).

Some molecular differences among *J. communis* populations support a recent colonization scenario (Vargas 2003; Mao et al., 2010; Adams et al., 2011). An early-diverging haplotype of *J. communis* distributed in Central Asia and the Himalayas region further corroborates this hypothesis (Hantemirova et al., 2017). While Mao et al. (2010) suggested that the European *J. communis* populations were phylogenetically closer to the American than to the Asian ones, recent research using nuclear microsatellite markers found no significant differences between the Alaskan and East Asian samples (Hantemirova and Bessonova, 2023). That is, although the migration routes of this circumboreal species deserve further research, colonization of North America likely occurred from eastern Asia through the Bering Land Bridge.

#### 4.3. Biogeographic history of Red cones species across the Mediterranean–Macaronesian regions

Boratyński et al. (2014), building on Mao et al. (2010)'s findings, proposed separate colonization events across the western and eastern Mediterranean basin by the ancestral lineage of the Red Cone clade. In this framework, speciation gave rise to *J. deltooides* and *J. oxycedrus* on opposite sides of the Mediterranean basin. Although the higher genetic diversity found in western than in eastern populations for several junipers (i.e. *J. oxycedrus* vs. *J. deltooides*; *J. macrocarpa* WM vs. *J. macrocarpa* EM) had led to hypothesize the western Mediterranean origin of this clade (Boratyński et al., 2014), our research suggests a more complete history of the Red Cones species. We identified two distinct lineages: the BND clade (*J. brevifolia*, *J. navicularis* and *J. deltooides*) and the *J. oxycedrus* clade (*J. oxycedrus* and allies plus *J. macrocarpa*). While the BND spans both sides of the Mediterranean basin and the Azores, *J. oxycedrus* and allies (*J. cedrus*, *J. badia*, *J. maderensis* and *J. oxycedrus*) are restricted to the western Mediterranean area the Canarian and Madeiran archipelagos. Considering that the crown node of the BND clade dates back to ca. 11.7 Ma, preceding the split of *J. oxycedrus* by about 4.5 Ma, and that the early diverging taxa from both clades are found in the eastern Mediterranean area, we propose two east-to-west colonization events across the Mediterranean area.

The first east-to-west colonization likely involved an ancestral lineage of the BND clade, giving rise to the present-day *J. brevifolia* and *J. navicularis*, currently limited to the southeastern Iberian Peninsula and the Azores, respectively. At the same time, the lineage of *J. deltooides*—the earliest-diverging species within the BND clade—, may have originated and diversified in the eastern Mediterranean area.

The disjunct distribution of the BND species could be explained by a progressive aridification during the Late Miocene, preceding the Messinian Salinity Crisis (MSC: 5.96–5.3 Ma; Krijgsman et al., 1999). Similarly to *Laurus* L., considered a sclerophyllous broad-leaved element from the Tethyan flora (Rodríguez-Sánchez et al., 2009), range fragmentation during the Miocene and Pliocene may have reduced the distribution range of the ancestral lineage of the BND clade in the western Mediterranean. Thus, high extinction rates of sclerophyllous taxa during the Pliocene/Pleistocene transition (Herrera, 1992; Verdú and Pausas, 2013) would have led to the current narrow endemic distribution range of the western Mediterranean members of the BND clade.

*Juniperus macrocarpa*, the most widely distributed species in the *J. oxycedrus* clade, spans the entire Mediterranean basin, while other taxa in this clade are native to the western Mediterranean and the Macaronesia. The early-diverging *J. macrocarpa* EM lineage (Figs. 1, 2) supports a second east-to-west juniper colonization of the Mediterranean basin. *Juniperus macrocarpa* inhabit coastal dunes and likely possesses salt and drought stress adaptations (Géhu et al., 1990; Muñoz-Reinoso, 2003) favoring the diversification of the ancestral *J. oxycedrus* clade in the western Mediterranean before and during the MSC, like others salt tolerant xerophytes such as *Haplophyllum* A. Juss. (Manafzadeh et al., 2014) and *Limonium* Mill. (Koutroumpa et al., 2021). Then, a colonization process may have occurred from the coastal habitats to the inland prior to the divergence of *J. oxycedrus* and *J. badia* around 7 and 5.5 Ma, respectively. The aridification of this period could have led to habitat reduction and vicariance resulting in the current taxa *J. oxycedrus* and *J. badia*. The sister relationship of the latter species with the clade containing *J. cedrus* and *J. maderensis*, suggests northern Africa as a possible geographic origin for *J. badia*.

Our findings support a stepping-stone history for the colonization of the Azorean archipelago (Rumeu et al., 2011) by an ancestral lineage of the BND clade, dated to around 9.5 Ma prior to the emergence of the oldest island Santa Maria (8.12 Ma). However, in contrast to previous findings (Rumeu et al. 2014), our analysis reveals a sister clade relationship between *J. cedrus* and *J. maderensis*, the southernmost Macaronesian junipers (see Figs. 1, 2). This evidence suggests two independent colonization events of the Macaronesian region: one

involving *J. brevifolia* in the Azores, and another linked to the evolutionary history of *J. cedrus* and *J. maderensis* in the Canary and Madeiran islands, respectively. That is, the three Macaronesian junipers (i.e. *J. brevifolia*, *J. cedrus* and *J. maderensis*) are examples of a single archipelago colonization, as observed in other Macaronesian species (e.g., Francisco-Ortega et al. 1996, Kim et al. 1996, Hess et al. 2000), but they never diversified within the archipelago (Patiño et al., 2014; Gallego-Narbón et al. 2023). The fact that junipers are bird-dispersed (high dispersal and gene flow) may help to explain that the first arrival quickly preempt all habitable space in the archipelagos.

#### 4.4. Conclusions

Our fully resolved phylogeny of the needle-leaved junipers (*J. sect. Juniperus*) based on GBS data provides robust evidence on the complex biogeographical history shaped by major geological and climatic events. We identified the Mediterranean basin as a primary center of diversification, followed by secondary diversification in East Asia, with a clear disjunction between both centers that were later connected by the expansion of the circumboreal species *J. communis*. It also shed light on the Systematics of the group, supporting the monophyly of both the Blue Cone and Red Cone groups in addition to the recognition of three taxa at the species taxonomic rank: *J. badia*, *J. conferta*, and *J. lutchuensis*.

#### CRedit authorship contribution statement

**David Gutiérrez-Larruscain:** Writing – original draft, Visualization, Validation, Investigation, Formal analysis, Conceptualization. **Pablo Vargas:** Writing – review & editing, Resources, Conceptualization. **Mario Fernández-Mazuecos:** Writing – review & editing, Formal analysis. **Juli G. Pausas:** Writing – review & editing, Funding acquisition, Conceptualization.

#### Acknowledgments

This research was funded by the project FocScales (Prometeo/2021/040; Generalitat Valenciana). We thank E. Cano for his invaluable support during the laboratory work, L. Medina and the entire team at the MA herbarium for allowing us access to their specimens, M. Menezes de Sequeira fom UMad (Herbarium of the University of Madeira) and J. Riera from VAL for their support, E herbarium for sampling, and R. P. Adams for kindly providing us with plant material from BAYLU.

#### Data accessibility.

Raw GBS data was deposited at the NCBI SRA database under BioProject PRJNA1083777. Occurrence dataset used for the historical biogeography analysis is available under the following doi: doi: 10.15468/dd.4ps5n7.

#### Appendix A. Supplementary data

Supplementary data to this article can be found online at <https://doi.org/10.1016/j.ympbev.2024.108162>.

#### References

- Adams, R.P., 2000. Systematics of *Juniperus* section *Juniperus* based on leaf essential oils and random amplified polymorphic DNAs (RAPDs). *Biochem. Syst. Ecol.* 28, 515–528. [https://doi.org/10.1016/S0305-1978\(99\)00089-7](https://doi.org/10.1016/S0305-1978(99)00089-7).
- Adams, R.P., 2011. *Juniperus of the world: the genus Juniperus*. Trafford Publishing, Victoria BC.
- Adams, R.P., Demeke, T., 1993. Systematic relationships in *Juniperus* based on random amplified polymorphic DNAs (RAPDs). *Taxon* 42, 553–571. <https://doi.org/10.2307/1222534>.
- Adams, R.P., Morris, J.A., Pandey, R.N., Schwarzbach, A.E., 2005. Cryptic speciation between *Juniperus deltooides* and *Juniperus oxycedrus* (Cupressaceae) in the Mediterranean. *Biochem. Syst. Ecol.* 33, 771–787. <https://doi.org/10.1016/j.bse.2005.01.001>.

- Adams, R.P., Fontinha, S.S., Rumeu, B., Nogales, M., 2010. Speciation of *Juniperus cedrus* and *J. maderensis* in the archipelagos of canaries and madeira based on terpenoids and nrDNA and petN-psbM sequences. *Phytologia* 92, 44–55.
- Adams, R.P., Murata, J., Takahashi, K., Schwarzbach, A.E., 2011. Taxonomy and evolution of *Juniperus communis*: insight from DNA sequencing and SNPs. *Phytologia* 93, 185–197.
- Adams, R.P., Schwarzbach, A.E., 2012. Taxonomy of *Juniperus*, section *Juniperus*: sequence analysis of nrDNA and five cpDNA regions. *Phytologia* 94, 280–297.
- Adams, R.P., Schwarzbach, A.E., 2013. Phylogeny of *Juniperus* using nrDNA and four cpDNA regions. *Phytologia* 95, 202–209.
- Almerikova, S., Yermagambetova, M., Abugalieva, S., Turuspekov, Y., 2022. The complete chloroplast genome sequencing data of *Juniperus sabina* L. (cupressaceae Bartl.) from Kazakhstan. *Data Brief* 45, 108644. <https://doi.org/10.1016/j.dib.2022.108644>.
- Amaral Franco, J., 1986. In: Castroviejo, S., Laínz, M., López González, G., Montserrat, P., Muñoz Garmendia, F., Paiva, L., Villar, L. (Eds.), *Flora Iberica*, Vol. 1. Real Jard. Bot. Madrid.
- Antoine, F., 1857. *Die Cupressineen-Gattungen: arceuthos. Juniperus und Sabina*. Friedrich Beck'schen Universitäts-Buchhandlung, Wien.
- Axelrod, D.I., 1975. Evolution and biogeography of medrean-tethyan sclerophyll vegetation. *Ann. Missouri Bot. Gard.* 62, 280–334.
- Ayres, D.L., Darling, A., Zwickl, D.J., Beerli, P., Holder, M.T., Lewis, P.O., Huelsenbeck, J.P., Ronquist, F., Swofford, D.L., Cummings, M.P., Rambaut, A., Suchard, M.A., 2012. BEAGLE: An application programming interface and high-performance computing library for statistical phylogenetics. *Syst. Biol.* 61, 170–173. <https://doi.org/10.1093/sysbio/syr100>.
- Boratyński, A., Wachowiak, W., Dering, M., Boratyńska, K., Sękiewicz, K., Sobierajska, K., Jasińska, A.K., Klimko, M., Montserrat, J.M., Romo, A., Ok, T., Didukh, Y., 2014. The biogeography and genetic relationships of *Juniperus oxycedrus* and related taxa from the Mediterranean and macaronesian regions: biogeography of *Juniperus Oxycedrus*. *Bot. J. Linn. Soc.* 174, 637–653. <https://doi.org/10.1111/boj.12147>.
- Bueno-Hernández, A., Barahona, A., Morronoe, J.J., Espinosa, D., Juárez-Barrera, F., 2023. Historiographical approaches to biogeography: a critical review. *Hist. Philos. Life Sci.* 45, 27. <https://doi.org/10.1007/s40656-023-00580-9>.
- Chen, C., Qi, Z., Xu, X., Comes, H.P., Koch, M.A., Jin, X., Fu, C., Qiu, Y., 2014. Understanding the formation of Mediterranean–African–Asian disjunctions: evidence for Miocene climate-driven vicariance and recent long-distance dispersal in the Tertiary relict *Smilax aspera* (Smilacaceae). *New Phytol.* 204, 243–255. <https://doi.org/10.1111/nph.12910>.
- Chernomor, O., Haeseler, A., Minh, B.Q., 2016. Terrace aware data structure for phylogenomic inference from supermatrices. *Syst. Biol.* 65, 997–1008. <https://doi.org/10.1093/sysbio/syw037>.
- Condamine, F.L., Silvestro, D., Koppelhus, E.B., Antonelli, A., 2020. The rise of angiosperms pushed conifers to decline during global cooling. *Proc. Natl. Acad. Sci. u.s.a.* 117, 28867–28875. <https://doi.org/10.1073/pnas.2005571117>.
- Costa, F.P., Schrago, C.G., Mello, B., 2022. Assessing the relative performance of fast molecular dating methods for phylogenomic data. *BMC Genomics* 23, 1–10. <https://doi.org/10.1186/s12864-022-09030-5>.
- Crisp, M.D., Cook, L.G., 2011. Cenozoic extinctions account for the low diversity of extant gymnosperms compared with angiosperms. *New Phytol.* 192, 997–1009. <https://doi.org/10.1111/j.1469-8137.2011.03862.x>.
- Davis, C.C., Schaefer, B., 2011. Plant Evolution: pulses of extinction and speciation in gymnosperm diversity. *Curr. Biol.* 21, R995–R998. <https://doi.org/10.1016/j.cub.2011.11.020>.
- Deng, T., Zhang, J.-W., Meng, Y., Volis, S., Sun, H., Nie, Z.-L., 2017. Role of the Qinghai-Tibetan Plateau uplift in the Northern Hemisphere disjunction: evidence from two herbaceous genera of Rubiaceae. *Sci. Rep.* 7, 13411. <https://doi.org/10.1038/s41598-017-13543-5>.
- Doyle, J.J., Doyle, J.L., 1987. A Rapid DNA isolation procedure for small quantities of fresh leaf tissue. *Phytochem. Bull.* 19, 11–15.
- Eaton, D.A.R., Overcast, I., 2020. Ipyrad: Interactive assembly and analysis of RADseq datasets. *Bioinformatics* 36, 2592–2594. <https://doi.org/10.1093/bioinformatics/btz966>.
- Elshire, R.J., Glaubitz, J.C., Sun, Q., Poland, J.A., Kawamoto, K., Buckler, E.S., Mitchell, S.E., 2011. A robust, simple genotyping-by-sequencing (GBS) approach for high diversity species. *PLoS One* 6, 1–10. <https://doi.org/10.1371/journal.pone.0019379>.
- Emerson, B.C., Hewitt, G.M., 2005. Phylogeography. *Curr. Biol.* 15, 367–371. <https://doi.org/10.1016/j.cub.2005.05.016>.
- Endlicher, S., 1847. *Synopsis coniferarum*. Apud Scheitlin & Zollikofer, Sangalli (Switzerland).
- Escudero, M., Eaton, D.A.R., Hahn, M., Hipp, A.L., 2014. Genotyping-by-sequencing as a tool to infer phylogeny and ancestral hybridization: a case study in *Carex* (Cyperaceae). *Mol. Phylogenet. Evol.* 79, 359–367. <https://doi.org/10.1016/j.ympbev.2014.06.026>.
- Farhat, P., Siljak-Yakovlev, S., Takvorian, N., Bou Dagher Kharrat, M., Robert, T., 2023. Allopolyploidy: An Underestimated Driver in *Juniperus* Evolution. *Life* 13, 1479. [doi: 10.3390/life13071479](https://doi.org/10.3390/life13071479).
- Farhat, P., Hidalgo, O., Robert, T., Siljak-Yakovlev, S., Leitch, I.J., Adams, R.P., Bou Dagher-Kharrat, M., 2019. Polyploidy in the Conifer genus *Juniperus*: an unexpectedly high rate. *Front. Plant Sci.* 10, 676. <https://doi.org/10.3389/fpls.2019.00676>.
- Farjon, A., 2001. *World Checklist and bibliography of conifers*. Royal Botanic Gardens, Kew.

- Farjon, A., 2005. A monograph of Cupressaceae and Sciadopitys. Royal Botanic Gardens, Kew.
- Farjon, A., 2017. A Handbook of the world's conifers, 2nd ed. Brill, Leiden.
- Fernández-Mazuecos, M., Mellers, G., Vignalondo, B., Sáez, L., Vargas, P., Glover, B.J., 2018. Resolving Recent plant radiations: power and robustness of genotyping-by-sequencing. *Syst. Biol.* 67, 250–268. <https://doi.org/10.1093/sysbio/syx062>.
- Francisco-Ortega, J., Jansen, R.K., Santos-Guerra, A., 1996. Chloroplast DNA evidence of colonization, adaptive radiation, and hybridization in the evolution of the Macaronesian flora. *Proc. Natl. Acad. Sci. U.S.A.* 93, 4085–4090. <https://doi.org/10.1073/pnas.93.9.4085>.
- Gallego-Narabón, A., Alonso, A., Varcárcel, V., Fernández-Mazuecos, M., 2023. Repeat asynchronous evolution of single-species endemics of ivies (*Hedera* L.) in Macaronesian archipelagos. *J. Biogeogr.* 50, 1763–1777. <https://doi.org/10.1111/jbi.14690>.
- H. Gay Sur quelques plantes intéressantes M.G. Masson Rares Ou Nouvelles De La Flore D'algerie, et Spécialement De La Région Méditerranéenne, in: Comptes Rendus De L'association Française Pour L'avancement Des Sciences - Notes et Mémoires 1889 Paris 499 507.
- Géhu, J.M., Costa, M., Biondi, E., 1990. Les Junipereta Macrocarpae Sur Sable. *ABM* 15, 303–309. <https://doi.org/10.24310/abm.v15i.9313>.
- Guindon, S., Dufayard, J.F., Lefort, V., Anisimova, M., Hordijk, W., Gascuel, O., 2010. New Algorithms and Methods to Estimate maximum-likelihood phylogenies: assessing the performance of PhyML 3.0. *Syst. Biol.* 59, 307–321. <https://doi.org/10.1093/sysbio/syq010>.
- Hamon, P., Grover, C.E., Davis, A.P., Rakotomalala, J.J., Raharimalala, N.E., Albert, V. A., Sreenath, H.L., Stoffelen, P., Mitchell, S.E., Couturon, E., Hamon, S., de Kochko, A., Crouzillat, D., Rigoreau, M., Sumirat, U., Akaffou, S., Guyot, R., 2017. Genotyping-by-sequencing provides the first well-resolved phylogeny for coffee (*Coffea*) and insights into the evolution of caffeine content in its species: GBS coffee phylogeny and the evolution of caffeine content. *Mol. Phylogenet. Evol.* 109, 351–361. <https://doi.org/10.1016/j.ympev.2017.02.009>.
- Hantemirova, E.V., Bessonova, V.A., 2023. Genetic Diversity of *Juniperus communis* L. in eurasia and alaska inferred from nuclear microsatellite markers. *Russ. J. Genet.* 59, 271–280. <https://doi.org/10.1134/S1022795423030055>.
- Hantemirova, E.V., Heinze, B., Knyazeva, S.G., Musae, A.M., Lascoux, M., Semerikov, V. L., 2017. A new Eurasian phylogeographical paradigm? Limited contribution of southern populations to the recolonization of high latitude populations in *Juniperus communis* L. (Cupressaceae). *J. Biogeogr.* 44, 271–282. <https://doi.org/10.1111/jbi.12867>.
- Herrera, C.M., 1992. Historical Effects and sorting processes as explanations for contemporary ecological patterns: character syndromes in mediterranean woody plants. *Am. Nat.* 140, 421–446. <https://doi.org/10.1086/285420>.
- Hess, J., Kaderleit, J.W., Vargas, P., 2000. The colonization history of *Olea europaea* L. in Macaronesia based on internal transcribed spacer 1 (ITS-1) sequences, randomly amplified polymorphic DNAs (RAPD), and interspersed sequence repeats (ISSR). *Mol. Ecol.* 9, 857–868. <https://doi.org/10.1046/j.1365-294x.2000.00942.x>.
- Hoang, D.T., Chernomor, O., von Haeseler, A., Minh, B.Q., Vinh, L.S., 2018. UFBBoot2: Improving the Ultrafast Bootstrap Approximation. *molecular biology and evolution.* *Mol. Biol. Evol.* 35, 518–522. <https://doi.org/10.5281/zenodo.854445>.
- Hühn, P., Dillenberger, M.S., Gerschütz-Eidt, M., Hörandl, E., Los, J.A., Messerschmid, T.F.E., Paetzold, C., Rieger, B., Kaderleit, G., 2022. How challenging RADseq data turned out to favor coalescent-based species tree inference. a case study in Aichryson (Crassulaceae). *Mol. Phylogenet. Evol.* 167 <https://doi.org/10.1016/j.ympev.2021.107342>.
- Jiang, X., Hipp, A.L., Deng, M., Su, T., Zhou, Z., Yan, M., 2019. East Asian origins of European holly oaks (*Quercus* section *Ilex* Loudon) via the Tibet-Himalaya. *J. Biogeogr.* 46, 2203–2214. <https://doi.org/10.1111/jbi.13654>.
- Kalyaanamoorthy, S., Minh, B.Q., Wong, T.K.F., von Haeseler, A., Jermini, L.S., 2017. ModelFinder: fast model selection for accurate phylogenetic estimates. *Nat. Methods* 14, 587–589. <https://doi.org/10.1038/nmeth.4285>.
- Kim, S.C., Crawford, D.J., Francisco-Ortega, J., Santos-Guerra, A., 1996. A common origin for woody sonchus and five related genera in the Macaronesian islands: molecular evidence for extensive radiation. *Proc. Natl. Acad. Sci. U.S.A.* 93, 7743–7748. <https://doi.org/10.1073/pnas.93.15.7743>.
- Koutroumpa, K., Warren, B.H., Theodoridis, S., Coiro, M., Romeiras, M.M., Jiménez, A., Conti, E., 2021. Geo-Climatic Changes and Apomixis as major drivers of diversification in the mediterranean sea lavenders (*Limonium* Mill.). *Front. Plant Sci.* 11, 612258 <https://doi.org/10.3389/fpls.2020.612258>.
- Krijgsman, W., Hilgen, F.J., Raffi, I., Sierro, F.J., Wilson, D.S., 1999. Chronology, causes and progression of the Messinian salinity crisis. *Nature* 400, 652–655. <https://doi.org/10.1038/23231>.
- Kvaček, Z., 1999. An ancient calocedrus (Cupressaceae) from the European tertiary. *Flora* 194, 237–248. [https://doi.org/10.1016/S0367-2530\(17\)30902-7](https://doi.org/10.1016/S0367-2530(17)30902-7).
- Kvaček, Z., 2002. A new juniper from the Palaeogene of Central Europe. *Feddes Repertorium* 113, 492–502. <https://doi.org/10.1002/fedr.200290001>.
- Kvaček, Z., Manchester, S.R., Schorn, H.E., 2000. Cones, seeds, and foliage of *Tetraclinis salicornioides* (Cupressaceae) from the oligocene and Miocene of Western North America: a geographic extension of the European tertiary species. *Int. J. Plant Sci.* 161, 331–344. <https://doi.org/10.1086/314245>.
- Li, S.-F., Valdes, P.J., Farnsworth, A., Davies-Barnard, T., Su, T., Lunt, D.J., Spicer, R.A., Liu, J., Deng, W.-Y., Huang, J., Tang, H., Ridgwell, A., Chen, L.-L., Zhou, Z.-K., 2021. Orographic evolution of northern Tibet shaped vegetation and plant diversity in eastern Asia. *Sci. Adv.* 7, eabc7741. <https://doi.org/10.1126/sciadv.abc7741>.
- Li, Y., Wang, L., Zhang, X., Kang, H., Liu, C., Mao, L., Fang, Y., 2022. Extensive sharing of chloroplast haplotypes among East Asian *Cerris* oaks: the imprints of shared ancestral polymorphism and introgression. *Ecol. Evol.* 12, e9142.
- Liang, H., Deng, J., Gao, G., Ding, C., Zhang, L., Xu, K., Wang, H., Yang, R., 2021. Inferring the phylogeny and divergence of chinese curcuma (Zingiberaceae) in the hengduan mountains of the qinghai-tibet plateau by reduced representation sequencing. *Forests* 12. <https://doi.org/10.3390/f12050520>.
- Liu, X., Yin, Z.-Y., 2002. Sensitivity of East Asian monsoon climate to the uplift of the Tibetan Plateau. *Palaeogeogr. Palaeoclimatol. Palaeoecol.* 183, 223–245. [https://doi.org/10.1016/S0031-0182\(01\)00488-6](https://doi.org/10.1016/S0031-0182(01)00488-6).
- Maestri, R., Duarte, L., 2020. Evoregions: Mapping shifts in phylogenetic turnover across biogeographic regions. *Methods Ecol. Evol.* 11, 1652–1662. <https://doi.org/10.1111/2041-210X.13492>.
- Manafzadeh, S., Salvo, G., Conti, E., 2014. A tale of migrations from east to west: the Irano-Turanian floristic region as a source of Mediterranean xerophytes. *J. Biogeogr.* 41, 366–379. <https://doi.org/10.1111/jbi.12185>.
- Mao, K., Hao, G., Liu, J., Adams, R.P., Milne, R.I., 2010. Diversification and biogeography of *Juniperus* (Cupressaceae): Variable diversification rates and multiple intercontinental dispersals. *New Phytol.* 188, 254–272. <https://doi.org/10.1111/j.1469-8137.2010.03351.x>.
- Martínez-Rodríguez, J., Vargas, P., 2022. High plastid (trnL-F) sequence variation in *Juniperus* sect. *Juniperus* reveals active dispersal across the Mediterranean and Macaronesia [study finished in 2010]. *DIGITAL.CSIC*. doi: 10.20350/digitalCSIC/14881.
- Martín-Hernanz, S., Aparicio, A., Fernández-Mazuecos, M., Rubio, E., Reyes-Betancort, J. A., Santos-Guerra, A., Olangua-Corral, M., Albaladejo, R.G., 2019. Maximize Resolution or Minimize Error? Using Genotyping-By-Sequencing to investigate the Recent diversification of helianthemum (Cistaceae). *Front. Plant Sci.* 10, 1–21. <https://doi.org/10.3389/fpls.2019.01416>.
- Matzke, M.J., 2014. Model Selection in Historical Biogeography reveals that founder-event speciation is a crucial process in island clades. *Syst. Biol.* 63, 951–970. <https://doi.org/10.1093/sysbio/syu056>.
- McDowall, R.M., 1978. Generalized tracks and dispersal in biogeography. *Syst. Zool.* 27, 88. <https://doi.org/10.2307/2412819>.
- Minh, B.Q., Hahn, M.W., Lanfear, R., 2020a. New methods to calculate concordance factors for phylogenomic datasets. *Mol. Biol. Evol.* 37, 2727–2733. <https://doi.org/10.1093/molbev/msaa106>.
- Minh, B.Q., Schmidt, H.A., Chernomor, O., Schrempf, D., Woodhams, M.D., Von Haeseler, A., Lanfear, R., Teeling, E., 2020b. IQ-TREE 2: New Models and Efficient Methods for Phylogenetic Inference in the Genomic Era. *Mol. Biol. Evol.* 37, 1530–1534. <https://doi.org/10.1093/molbev/msaa015>.
- Muñoz-Reinos, J.C., 2003. *Juniperus oxycedrus* ssp. *macrocarpa* in SW Spain: ecology and conservation problems. *J. Coast. Conserv.* 9, 113–122. <https://doi.org/10.1007/BF02838082>.
- Naciri, Y., Linder, H.P., 2015. Species delimitation and relationships: the dance of the seven veils. *Taxon* 64, 3–16. <https://doi.org/10.12705/641.24>.
- Nagalingum, N.S., Marshall, C.R., Quental, T.B., Rai, H.S., Little, D.P., Mathews, S., 2011. Recent Synchronous Radiation of a Living Fossil. *Science* 334, 796–799. <https://doi.org/10.1126/science.1209926>.
- Nakamura, G., Rodrigues, A.V., Luza, A.L., Maestri, R., Debastiani, V., Duarte, L., 2023. Herodotools: an R package to integrate macroevolution, biogeography and community ecology. *J. Biogeogr.* jbi.14610 <https://doi.org/10.1111/jbi.14610>.
- Negru, A.G., 1972. Lower Sarmatian Flora of northeastern Moldavia. *Kishinev, Moldova, Shtiintsa*.
- Nelson, G., 1978. From Candolle to croizat: comments on the history of biogeography. *J. Hist Biol* 11, 269–305. <https://doi.org/10.1007/BF00389302>.
- Nelson, G., Patnick, N., 1981. *Systematics and Biogeography: cladistics and Vicariance*. Columbia University Press, New York.
- Otero, A., Vargas, P., Fernández-Mazuecos, M., Jiménez-Mejías, P., Valcárcel, V., Villamachío, I., Hipp, A.L., 2022. A snapshot of progenitor-derivative speciation in Iberodes (Boraginaceae). *Mol. Ecol.* 31, 3192–3209. <https://doi.org/10.1111/mec.16459>.
- Palamarev, E., 1989. Paleobotanical evidences of the Tertiary history and origin of the Mediterranean sclerophyll dendroflora. *Pl. Syst. Evol.* 162, 93–107. <https://doi.org/10.1007/BF00936912>.
- Palamarev, E., Bozukov, V., Uzunova, K., Petkova, A., Kitanov, G., 2005. Catalogue of the cenozoic plants of bulgaria (Eocene to Pliocene). *Phytol. Bal.* 11, 215–364.
- Patiño, J., Carine, M., Fernández-Palacios, J.M., Otto, R., Schaefer, H., Vanderpoorten, A., 2014. The anagenetic world of spore-producing land plants. *New Phytol.* 201, 305–311. <https://doi.org/10.1111/nph.12480>.
- Queiroz, A., 2005. The resurrection of oceanic dispersal in historical biogeography. *TREE* 20, 68–73. <https://doi.org/10.1016/j.tree.2004.11.006>.
- Raven, P.H., 1972. Plant Species disjunctions: a summary. *Ann. Missouri Bot. Gard.* 59, 234. <https://doi.org/10.2307/2394756>.
- Rivas, S., Molero, J., Marfil, J.M., Benítez, G., 2020. Floristic and geobotanical comments concerning Morocco flora. *Note. Nat. Cantabr.* 8, 115–121.
- Rodríguez-Sánchez, F., Guzmán, B., Valido, A., Vargas, P., Arroyo, J., 2009. Late Neogene history of the laurel tree (*Laurus* L., Lauraceae) based on phylogeographical analyses of Mediterranean and Macaronesian populations. *J. Biogeogr.* 36, 1270–1281. <https://doi.org/10.1111/j.1365-2699.2009.02091.x>.
- Ronquist, F., Teslenko, M., Van Der Mark, P., Ayres, D.L., Darling, A., Höhna, S., Larget, B., Liu, L., Suchard, M.A., Huelsenbeck, J.P., 2012. MrBayes 3.2: Efficient bayesian phylogenetic inference and model choice across a large model space. *Syst. Biol.* 61, 539–542. <https://doi.org/10.1093/sysbio/sys029>.
- Rumeu, B., Caujapé-Castells, J., Blanco-Pastor, J.L., Jaén-Molina, R., Nogales, M., Elias, R.B., Vargas, P., 2011. The Colonization History of *Juniperus brevifolia* (Cupressaceae) in the Azores Islands. *PLoS ONE* 6, e27697. <https://doi.org/10.1371/journal.pone.0027697>.

- Rumeu, B., Vargas, P., Jaén-Molina, R., Nogales, M., Caujapé-Castells, J., 2014. Phylogeography and genetic structure of the threatened canarian juniperus cedrus (Cupressaceae). *Bot. J. Linn. Soc.* 175, 376–394. <https://doi.org/10.1111/boj.12172>.
- Sayyari, E., Mirarab, S., 2016. Fast Coalescent-based computation of local branch support from quartet frequencies. *Mol. Biol. Evol.* 33, 1654–1668. <https://doi.org/10.1093/MOLBEV/MSW079>.
- Shafer, A.B.A., Peart, C.R., Tusso, S., Maayan, I., Brelsford, A., Wheat, C.W., Wolf, J.B.W., 2017. Bioinformatic processing of RAD-seq data dramatically impacts downstream population genetic inference. *Methods Ecol. Evol.* 8, 907–917. <https://doi.org/10.1111/2041-210X.12700>.
- Sibthorp, J., Smith, J.E., 1816. *Florae Graecae prodromus; sive Plantarum omnium enumeratio*. Richard Taylor & Co., London.
- Solis-Lemus, C., Ané, C., 2016. Inferring Phylogenetic networks with maximum pseudolikelihood under incomplete lineage sorting. *PLoS Genet.* 12, e1005896.
- Solis-Lemus, C., Bastide, P., Ané, C., 2017. PhyloNetworks: a package for phylogenetic networks. *MBE* 34, 3292–3298. <https://doi.org/10.1093/molbev/msx235>.
- Spicer, R.A., Su, T., Valdes, P.J., Farnsworth, A., Wu, F.-X., Shi, G., Spicer, T.E.V., Zhou, Z., 2021. Why 'the uplift of the Tibetan Plateau' is a myth. *Natl. Sci.* 8, nwa091. <https://doi.org/10.1093/nsr/nwa091>.
- Steenwyk, J.L., Li, Y., Zhou, X., Shen, X., Rokas, A., 2023. Incongruence in the phylogenomics era. *Nat. Rev. Genet.* 24, 834–850. <https://doi.org/10.1038/s41576-023-00620-x>.
- Su, T., Farnsworth, A., Spicer, R.A., Huang, J., Wu, F.-X., Liu, J., Li, S.-F., Xing, Y.-W., Huang, Y.-J., Deng, W.-Y.-D., Tang, H., Xu, C.-L., Zhao, F., Srivastava, G., Valdes, P. J., Deng, T., Zhou, Z.-K., 2019. No high tibetan plateau until neogene. *Sci. Adv.* 5, eaav2189. <https://doi.org/10.1126/sciadv.aav2189>.
- Tamura, K., Battistuzzi, F.U., Billings-Ross, P., Murillo, O., Filipiński, A., Kumar, S., 2012. Estimating divergence times in large molecular phylogenies. *Proc. Natl. Acad. Sci. U. S. A.* 109, 19333–19338. <https://doi.org/10.1073/pnas.1213199109>.
- Tamura, K., Tao, Q., Kumar, S., 2018. Theoretical foundation of the realtime method for estimating divergence times from variable evolutionary rates. *Mol. Biol. Evol.* 35, 1770–1782. <https://doi.org/10.1093/molbev/msy044>.
- Tamura, K., Stecher, G., Kumar, S., 2021. MEGA11: molecular evolutionary genetics analysis version 11. *Mol. Biol. Evol.* 38, 3022–3027. <https://doi.org/10.1093/molbev/msab120>.
- Tu, T., Volis, S., Dillon, M.O., Sun, H., Wen, J., 2010. Dispersals of Hyoscyameae and Mandragoreae (Solanaceae) from the new world to eurasia in the early miocene and their biogeographic diversification within eurasia. *Mol. Phylogenetics Evol.* 57, 1226–1237. <https://doi.org/10.1016/j.ympev.2010.09.007>.
- Tumajer, J., Buras, A., Camarero, J.J., Carrer, M., Shetti, R., Wilmking, M., Altman, J., Sangüesa-Barreda, G., Leheček, J., 2021. Growing faster, longer or both? modelling plastic response of *Juniperus communis* growth phenology to climate change. *Global Ecol. Biogeogr.* 30, 2229–2244. <https://doi.org/10.1111/geb.13377>.
- Uckele, K.A., Adams, R.P., Schwarzbach, A.E., Parchman, T.L., 2021. Genome-wide RAD sequencing resolves the evolutionary history of the serrate leaf *Juniperus* and reveals discordance with chloroplast phylogeny. *Mol. Phylogenet. Evol.* 156, 107022.
- Valcárcel, V., Guzmán, B., Medina, N.G., Vargas, P., Wen, J., 2017. Phylogenetic and paleobotanical evidence for late Miocene diversification of the Tertiary subtropical lineage of ivies (*Hedera* L., Araliaceae). *BMC Evol. Biol.* 17, 146. <https://doi.org/10.1186/s12862-017-0984-1>.
- Van Dijk, A., Nakamura, G., Rodrigues, A.V., Maestri, R., Duarte, L., 2021. Imprints of tropical niche conservatism and historical dispersal in the radiation of Tyrannidae (Aves: Passeriformes). *Biol. J. Linn. Soc.* 134, 57–67. <https://doi.org/10.1093/biolinean/blab079>.
- Vargas, P., 2003. Molecular evidence for multiple diversification patterns of alpine plants in Mediterranean Europe. *Taxon* 52, 463–476. <https://doi.org/10.2307/3647383>.
- Verdú, M., Pausas, J.G., 2013. Syndrome-Driven diversification in a Mediterranean Ecosystem. *Evol.* 67, 1756–1766. <https://doi.org/10.1111/evo.12049>.
- Vilela, B., Villalobos, F., 2015. letsR: a new R package for data handling and analysis in macroecology. *Methods Ecol. Evol.* 6, 1229–1234. <https://doi.org/10.1111/2041-210X.12401>.
- Wagner, N.D., He, L., Hörandl, E., 2020. Phylogenomic Relationships and evolution of polyploid salix species revealed by RAD sequencing data. *Front. Plant Sci.* 11, 1–15. <https://doi.org/10.3389/fpls.2020.01077>.
- Wen-tsai, W., Wan-chün, C., Li-kuo, F., Cheng-de, C., 1978. Cupressaceae. In: Wan-chün, C., Li-kuo, F. (Eds.), *Flora Reipublicae Popularis Sinicae*. Science Press, Beijing, pp. 313–397.
- Wiley, E.O., 1988. Vicariance Biogeography. *Ann. Rev. Ecol. Syst.* 19, 513–542.
- Willkomm, H.M., 1852. *Sertum florae Hispanicae*. in Commission bei Joh. Friedr. Hartknoch. Leipzig.
- Xia, M., Cai, M., Comes, H.P., Zheng, L., Ohi-Toma, T., Lee, J., Qi, Z., Konowalik, K., Li, P., Cameron, K.M., Fu, C., 2022. An overlooked dispersal route of Cardueae (Asteraceae) from the Mediterranean to East Asia revealed by phylogenomic and biogeographical analyses of *Atractylodes*. *Ann. Bot.* 130, 53–64. <https://doi.org/10.1093/aob/mcac059>.
- Xie, L., Yang, Z.-Y., Wen, J., Li, D.-Z., Yi, T.-S., 2014. Biogeographic history of Pistacia (Anacardiaceae), emphasizing the evolution of the Madrean-Tethyan and the eastern Asian-Tethyan disjunctions. *Mol. Phylogenetics Evol.* 77, 136–146. <https://doi.org/10.1016/j.ympev.2014.04.006>.
- Yang, Y., Ferguson, D.K., Liu, B., Mao, K.S., Gao, L.M., Zhang, S.Z., Wan, T., Rushforth, K., Zhang, Z.X., 2022. Recent advances on phylogenomics of gymnosperms and a new classification. *Plant Divers.* 44, 340–350. <https://doi.org/10.1016/j.pld.2022.05.003>.
- Zhang, C., Rabiee, M., Sayyari, E., Mirarab, S., 2018. ASTRAL-III: polynomial time species tree reconstruction from partially resolved gene trees. *BMC Bioinf.* 19, 15–30. <https://doi.org/10.1186/s12859-018-2129-y>.
- Zhang, M.-L., Xiang, X.-G., Xue, J.-J., Sanderson, S.C., Fritsch, P.W., 2016. Himalayan uplift shaped biomes in Miocene temperate Asia: evidence from leguminous Caragana. *Sci. Rep.* 6, 36528. <https://doi.org/10.1038/srep36528>.
- Zhao, W., Gao, J., Hall, D., Andersson, B.A., Bruxaux, J., Tomlinson, K.W., Drouzas, A.D., Suyama, Y., Wang, X., 2024. Evolutionary radiation of the Eurasian *Pinus* species under pervasive gene flow. *New Phytol.* 242, 2353–2368. <https://doi.org/10.1111/nph.19694>.